Nuclear Instruments and Methods in Physics Research B 354 (2015) 332–339

Contents lists available at ScienceDirect

Nuclear Instruments and Methods in Physics Research B

journal homepage: www.elsevier.com/locate/nimb

High-energy electron scattering from TiO_2 surfaces

M. Vos [a,*], P.L. Grande [b]

[a] Atomic and Molecular Physics Laboratories, Research School of Physics and Engineering, The Australian National University, Canberra 0200, Australia
[b] Instituto de Fisica da Universidade Federal do Rio Grande do Sul, Avenida Bento Goncalves 9500, 91501-970 Porto Alegre, RS, Brazil

ARTICLE INFO

Article history:
Received 29 July 2014
Received in revised form 24 November 2014
Accepted 25 November 2014
Available online 16 December 2014

Keywords:
Electron Rutherford backscattering
TiO_2
Elastic cross sections
Dielectric function
Preferential sputtering

ABSTRACT

Electron scattering experiments at keV energies from a TiO_2 surface are presented. The paper aims to give an overview of the wide variety of information that can be extracted from such experiments. If the elastic scattering cross sections are known these experiments give the sample composition, if the composition is known one can extract the ratio of the elastic cross sections. In the experiments described here the ratio of the Ti and O cross sections deviates noticeably from the one calculated from the Rutherford formula. The peak widths give access to the mean kinetic energies of the atoms present. We show that the mean kinetic energy of Ti atoms is less than that of O atoms, but both kinetic energies are still affected by quantum effects, i.e. are larger than $3/2\,kT$. We extract an estimate of the dielectric function of TiO_2 by extending the measurement up to 100 eV energy loss. At these high energies the determination of the dielectric function from the measured energy loss spectrum is relatively simple, as the contribution of surface excitations is small and the obtained loss function is closely related to the dielectric function in the optical limit. Finally, we use the technique to monitor the surface after sputtering with Ar^+ ions, and observe both differences in composition and electronic structure induced by sputtering that disappear again after annealing.

1. Introduction

Large-angle scattering of keV electrons from surfaces at high energies provides a wealth of information. Under these conditions the recoil energies can be resolved, particularly for light atoms, and the technique is then usually referred to as electron Rutherford backscattering spectrometry (ERBS) [1,2]. As a consequence the elastic peak for compounds splits up into several components due to the different atomic constituents. Each component has a different intrinsic width, which is related to the momentum distribution of the scattering atom. Moreover, at larger energy losses we see the effect of electronic excitations. When these excitations are studied the spectroscopy is usually referred to as reflection electron energy loss spectroscopy (REELS). In REELS the elastic peak position is taken as the zero energy-loss position. This interpretation becomes ambiguous if the elastic peak splits up in several components of comparable magnitude. Such a case is TiO_2 where the oxygen elastic peak has ≈25% of the intensity of the Ti elastic peak. Here we present a subtraction procedure to remove this ambiguity. This procedure turns out to be competitive with a more traditional curve fitting approach for interpreting the elastic peak in terms of their separate components. The results show clearly that the differential elastic scattering cross sections (DCS) deviate significantly from those given by the Rutherford formula.

Both the experimental resolution and Doppler broadening due to atomic vibrations contribute to the elastic peak width. The experimental resolution is determined by evaporating a small amount of Au on the surface. This results in a third elastic peak (besides the ones due to Ti and O) but the intrinsic width of the Au peak is well-understood. It can thus be used to determine the spectrometer resolution. Provided with this information we are able to determine the mean kinetic energy of O and Ti atoms in TiO_2, which turns out to be significantly higher than what is expected in the classical limit: 3/2 kT. Surprisingly, few measurements exist of this basic quantity and we compare our results with some theoretical models.

Next we obtain an estimate of the dielectric function $\epsilon(k,\omega)$ for TiO_2 (where k is the momentum of the electronic excitation and ω the energy loss). Here several estimates already exist, but the theoretical and experimental estimates of this important property vary considerably. We argue that our measurement is close to the optical limit, and hence our estimate of the dielectric function at $k = 0$ should be quite reliable.

Finally it is demonstrated how one can monitor effects of sputtering with this technique. Ar ions remove preferentially O atoms.

* Corresponding author.
E-mail address: maarten.vos@anu.edu.au (M. Vos).

http://dx.doi.org/10.1016/j.nimb.2014.11.083
0168-583X/

As a consequence both changes in composition and electronic structure are observed, but the initial spectra are largely recovered after annealing.

This study is in many ways a follow-up of our work on HfO_2 and shows that much of the physics revealed for HfO_2 is also present for TiO_2. A more extensive discussion can often be found in the papers on HfO_2 [3–5].

2. Theory

Fast electrons (with energy E_0) moving through a material can lose energy by creating inelastic (i.e. electronic) excitations or change direction by deflection from a target atom. It is often assumed that the creation of inelastic excitation does not affect the direction of propagation of the electron, and that deflection from a target atom does not change its energy. Both assumptions are approximations only, the first one becomes better, the second one worse, with increasing E_0 values. The deflection from a nucleus results in a momentum transfer q to the scattering atom, and, if the atom was initially at rest, it acquires a kinetic energy $q^2/2M_i$ with M_i the mass of the atom i. If the atom had a momentum p before the collision, then the recoil energy E_r (i.e. the change kinetic energy of the atom due to the recoil) is given by:

$$E^i_{\rm rec} = \frac{(p+q)^2}{2M_i} - \frac{p^2}{2M_i} = \frac{q^2}{2M_i} + \frac{p\cdot q}{M_i}. \quad (1)$$

The projectile energy is reduced by this amount. The elastic peak is thus centred on the mean recoil energy $\overline{E^i_{\rm rec}} = q^2/2M_i$ but its shape is a Compton profile of the atomic motion. If the target contains two elements with substantially different masses M_i then the elastic peak splits up in two components, each related to a different element, and with a width that is determined by the momentum distribution of that element [1].

It can be shown that for isotropic targets (e.g. polycrystalline samples) the intrinsic width of a peak is related to the mean kinetic energy $\overline{E^i_{\rm kin}}$ of element i by the following equation [6]:

$$\sigma_i = \sqrt{\frac{4}{3}\overline{E^i_{\rm rec}}\,\overline{E^i_{\rm kin}}}. \quad (2)$$

In the previous we assumed implicitly that the scattering of an electron by an atom can be described as incoherent (the electron scatters from a single atom) and that the atom behaves as a free particle, i.e. we neglected the fact that the atom is bound to the target. Especially the latter assumption is far from obvious as the transferred energy is usually less than the binding energy of the atom. Nevertheless this assumption, referred to as the impulse approximation, works quite well under the present conditions. The impulse approximation is discussed extensively for neutron scattering at similar momentum transfers (then usually referred to as neutron Compton scattering) [7,8] which is in many ways the neutron-analogue of the present experiment.

For compounds the ratio for the elastic peaks is proportional to the relative concentration of the different elements *and* their DCS values. As a first approximation the DCS can be obtained from the Rutherford formula, but partial wave calculations [9] show that under these conditions the DCS for scattering of electrons from heavy atoms is enhanced relative to the Rutherford DCS values. For scattering from TiO_2 at 40 keV and 135° the expected elastic peak ratio for the partial wave cross sections differs by 10% from the expectations based on Rutherford, and the difference increases with decreasing E_0 values. For a target of known composition these measurements can thus be used to verify the partial wave calculations. Relevant values of the DCS are given in Table 1 as well as the mean recoil energy $\overline{E^i_{\rm rec}}$.

Table 1
The differential cross section as calculated from partial wave calculations as implemented in ELSEPA [9] for Ti and O at the energies indicated, as well as the ratio of their cross section. Note that this ratio is energy dependent and deviates from $(Z_{\rm Ti}/Z_{\rm O})^2 = 7.56$ as obtained for the Rutherford cross sections. The mean recoil energy $\overline{E^i_{\rm rec}}$ for scattering from Ti or O over 135° are given in the last columns.

E_0 (keV)	DCS O (cm^{-2})	DCS Ti (cm^{-2})	Ratio	$\overline{E^i_{\rm rec}}$ Ti (eV)	$\overline{E^i_{\rm rec}}$ O (eV)
5	5.04E−21	4.79E−20	9.50	0.20	0.59
25	1.82E−22	1.55E−21	8.51	1.00	3.00
40	6.93E−23	5.79E−22	8.35	1.62	4.86

An example of a spectrum of 40 keV electrons scattered over 135° from TiO_2 is given in Fig. 1. The two elastic peaks are followed by a feature-rich energy loss spectrum. In the following we try to uncover the information that is contained in such a spectrum.

3. Some experimental details

ERBS measurements were done with our spectrometer described extensively elsewhere, see e.g.[2,10]. Briefly, 40 keV electrons are scattered over 135° from a target and the scattered electrons are energy-analysed with a resolution of 0.3 eV. This is good enough to separate the contributions of Ti and O to the elastic peak and their intrinsic width. The zero point of the energy scale is not exactly known and we use the energy peak of the heaviest peak (in this case Ti) to fix the zero position by assuming that it has a recoil energy as calculated for an electron scattering from a free atom (1.62 eV for electrons scattering from free Ti under these conditions). When electronic excitations are studied it is more convenient to align the Ti peak with zero energy loss, as then the energy loss scale corresponds directly to the energy of the electronic excitation created.

The TiO_2 sample was grown by annealing a high-purity Ti foil for 5 h at 650 °C under a flow of high purity oxygen. The thickness of the polycrystalline (mainly rutile) oxide film grown in this way is several 1000 Å. For one experiment 2 Å of Au was evaporated from a W coil and the thickness was determined from a crystal thickness monitor reading.

4. Subtraction procedure for the contribution of electrons scattered from Oxygen

All detected electrons have been scattered elastically at least once, as inelastic excitations basically do not affect the direction of propagation of the projectile electron. The fact that we see two well-defined peaks in the spectra with a separation within 1–2% of what is predicted by Eq. (1) is a strong indication that the vast majority of detected electrons had basically a v-shaped trajectory with only a single large-angle elastic deflection. Assuming v-shaped trajectories and a *spatially homogeneous* target then for TiO_2 the spectrum can be separated into a part that is due to electrons scattered elastically from Ti and a part due to electrons scattered elastically from O. The intensity ratio of both contributions is determined by their relative concentration and the ratio of their DCS at the scattering angle dictated by the experimental geometry. Thus all detected electrons have lost energy due to the recoil, and many have lost additional energy due to inelastic excitations.

The contribution of electrons scattered elastically from O is shifted to larger energy losses by the difference of the Ti and O mean recoil energy. The Ti part of the spectrum is broadened by the Doppler broadening due to the Ti atom motion, whereas the O part is broadened by the Doppler broadening of the O atom. From Eq. (2) it is clear that for the lighter element the Doppler broaden-

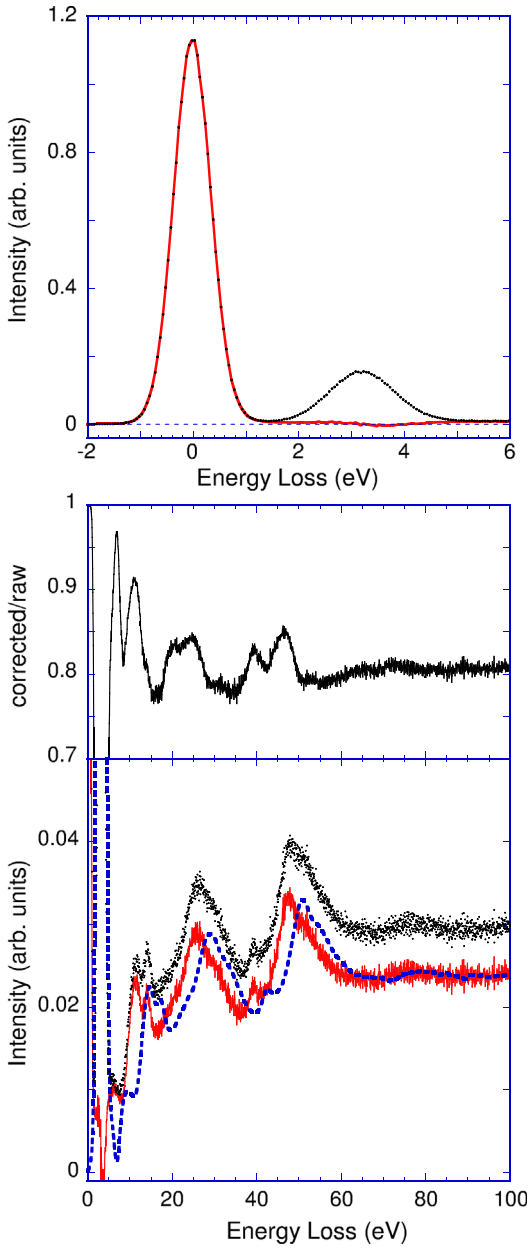

Fig. 1. A spectrum of a TiO_2 film. The top panel shows the elastic peak of Ti and O as measured (dots) and after subtraction of the contribution due to electrons scattering from oxygen (solid line). The subtraction procedure is described in Section 4. The bottom panel shows the energy loss spectrum over a much wider energy range. There are small changes in the shape of the energy loss spectrum before (black dots) and after (red line) subtraction of the contribution due to electrons scattered elastically from O atoms. This is emphasised in the central panel that shows the ratio of the signal before and after subtraction of the O-related intensity. Also plotted in the lower panel is the (scaled by ratio of the Ti and O DCS values) difference of the raw data and the spectrum after subtraction of the O contribution. It is the same distribution, but smoothed and shifted by the difference in recoil for Ti and O. (For interpretation of the references to colour in this figure legend, the reader is referred to the web version of this article.)

ing will be larger (as the recoil energy is larger) unless the kinetic energy of the heavier element exceeds that of the lighter element by a considerable factor. In practice one always find that the Doppler broadening is larger for the lighter elements. There is thus an ambiguity if one considers an energy loss spectrum of a compound taken under conditions where the recoil energy is resolved: the intensity at a certain energy loss can correspond to different electronic excitations, depending on the magnitude of the recoil energy. In the following a procedure is given to correct for this for homogeneous samples.

We start with an array $S[N]$ containing the spectrum including the elastic peaks and an array $E[N]$ containing the corresponding energy loss values, with subsequent elements increasing by E_{step}. We first consider the first element ($i = 1$) of this array (corresponding to the high kinetic energy side of the spectrum) and the intensity here ($S[i]$) is assumed to be only due to the electrons scattered from the heaviest element, in this case Ti. We define R as the ratio of the DCS values: $R = (\frac{d\sigma}{d\Omega})_O/(\frac{d\sigma}{d\Omega})_{Ti}$ and C as the ratio of number of O and Ti atoms present ($C = 2$ for TiO_2). There should be a contribution to the spectrum of magnitude RCS[i] due to electrons scattered from O at the array element j for which $E[j] \approx E[i] + \Delta E_{\text{rec}}/E_{\text{step}}$ with $\Delta E_{\text{rec}} = \overline{E_{\text{rec}}}(O) - \overline{E_{\text{rec}}}(Ti)$. However, the intensity of electrons scattered from O has a larger Doppler broadening ('extra width') than the intensity of electrons scattered from Ti. The intensity contribution RCS[i] is thus not just located at energy $E[i] + \Delta E_{\text{rec}}$ but distributed over a Gaussian centred at $E[i] + \Delta E_{\text{rec}}$. The width of this Gaussian, σ_{extra}, is given by $\sigma^2_{\text{extra}} = \sigma^2_O - \sigma^2_{Ti}$ where σ_{Ti} and σ_O refer to the intrinsic width of the Ti and O elastic peaks respectively. A spectrum S' can be obtained that is corrected for the O contribution related to the Ti intensity at $E[i]$ according to:

$$S'[j] = S[j] - \frac{\text{RCS}[i]}{\sqrt{2\pi}\sigma_{\text{extra}}} e^{-(E[j]-E[i]-\Delta E_{\text{rec}})^2/(2\sigma^2_{\text{extra}})} \quad (3)$$

for $j > i$ and $S'[j] = S[i]$ for $j \leqslant i$.

For the spectrum S' the O intensity is considered fully subtracted up to channel $i + 1$ and the procedure of Eq. (3) is repeated for $i = i + 1$ using S' as the input. By continuing in this way until $i = N$ the O contribution can be subtracted from the whole spectrum (both the elastic peak part and the energy loss part). An example of the result of the subtraction procedure is shown in Fig. 1.

The difference between the spectrum before and after the subtraction is of course the O contribution itself. Taking this difference (as is done in the lower panel of Fig. 1) and scaling it by the ratio of the Ti and O DCS values we get a spectrum that resembles that of the Ti only contribution, but is shifted by the difference in Ti and O recoil energies. Surprisingly, the O only contribution, obtained from subtracting two rather noisy spectra, is very smooth. Clearly the noise in the raw data, and the data after subtracting the O contribution is correlated. The procedure given in Eq. (3) smoothes the statistical noise further, as it effectively convolutes the Ti contribution with a Gaussian with a width σ_{extra}. Hence the O only contribution is proportional to the Ti only contribution shifted by the difference in recoil, but smoothed by a Gaussian function representing the difference in their Doppler broadening.

5. Results

We show the elastic peak area of a TiO_2 spectrum taken at E_0 values of 5, 25 and 40 keV in Fig. 2. For convenience the Ti peak is aligned with zero energy loss and is normalised to unit area. At 5 keV the Ti and O peaks are not resolved but the presence of O is still discernible as an asymmetry in the elastic peak. From the measurement with $E_0 = 5$ keV it is clear that the energy loss spectrum starts rising again a little over 3 eV, consistent with a band gap of 3.3 eV for rutile. This onset is obscured by the O elastic peak in the spectra taken with larger E_0 values. We now subtract the O contribution as described in Section 4. There are two parameters that affect the subtraction for which the values can be discussed: R and σ_{extra}. We used two values for R: the one expected based on the Rutherford formula ($R = Z^2_O/Z^2_{Ti}$) and the value calculated using the DCS as calculated by the partial wave method as implemented in ELSEPA [9] which, are reproduced in Table 1.

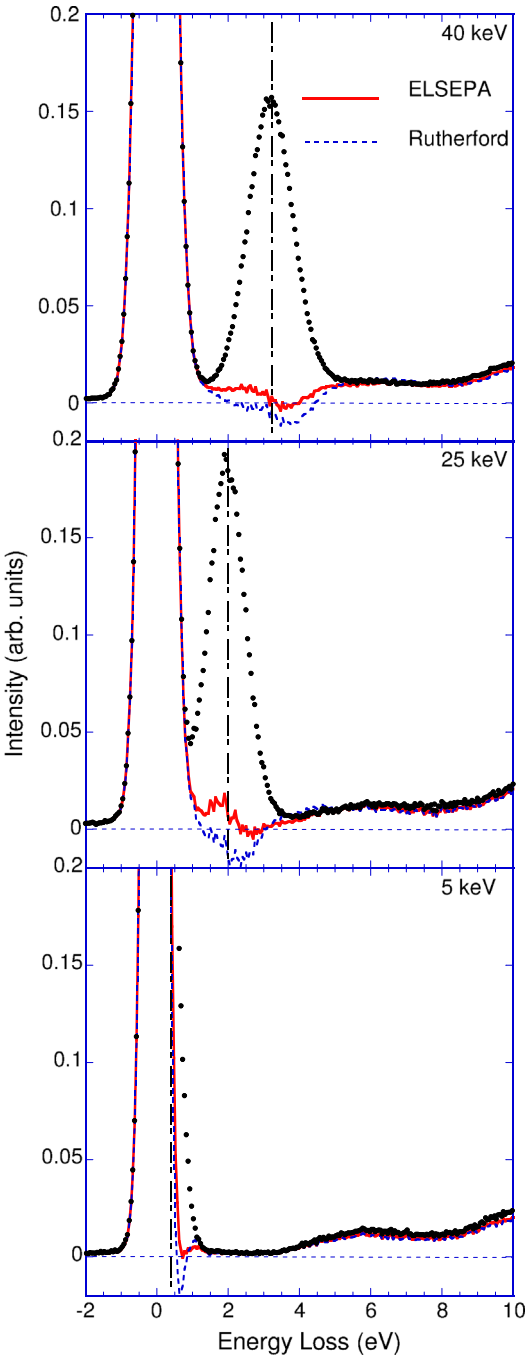

Fig. 2. Subtraction of the contribution of electrons scattered from oxygen from the spectrum of TiO_2, as energies of 40, 25 and 5 keV. The Ti peak is aligned with zero energy loss and the dashed line is the nominal O peak position. The intensity ratio of electrons scattered from O was taken to be that determined from the Rutherford formula (i.e. Z_1^2/Z_2^2, dashed line) or as calculated using ELSEPA (full line).

The best estimate for σ_{extra} was obtained by trial and error. The guiding principle is that the shape of the spectrum after subtraction of the O contribution should resemble the onset of the energy loss spectrum seen at 5 keV. A reasonable fit could only be obtained using the R values derived from ELSEPA. The R values based on Rutherford always produced significant negative intensities. We obtained values of $\sigma_{extra} = 0.51$ eV at 40 keV and 0.42 eV at 25 keV. Varying these values of σ_{extra} by more than 0.05 eV causes clear structure in the spectrum after subtraction.

Unfortunately the spectra after subtraction show still some structure that is not seen in the 5 keV energy loss spectrum. It is asymmetric relative to the O peak position, with excess intensity present at losses smaller than $\overline{E_{rec}}(O)$, and a deficit in intensity at larger losses. These residuals are very similar to those seen for electrons scattered from carbon at smaller momentum transfer [10] and for the H peak of gaseous spectra of CH_4 [11] and H_2O [12] at E_0 values around 1 keV. These deviations from a Gaussian line shape, similar to the ones seen here, were attributed to final state effects i.e. the failure of the assumption that we can treat the scattering atom as a free particle.

We also applied the procedure to the 5 keV spectrum. Here the O peak is not resolved, but still causes an asymmetry of the main elastic peak. After O peak subtraction the main peak becomes more symmetric. A value of 0.2 eV was used for σ_{extra}, but under these conditions we are not very sensitive to the exact value. The effect on the energy loss part of the spectrum is now very minor, as the recoil shift ΔE_{rec} is smaller than the width of the energy loss structures. Again using the R value derived from Rutherford cross sections (which deviate at these low energies substantially, i.e. by 25% from the ELSEPA value) one can not avoid negative intensities after subtraction.

From a TiO_2 spectrum as shown in Fig. 1 one cannot obtain estimates of the mean kinetic energy of Ti and O atoms, as the contribution of the spectrometer resolution to the observed widths is unknown. To remediate this we evaporated 2 Å of Au on the TiO_2 surface. Au is a soft metal with a low Debye temperature (170 K). Hence we are confident that the mean kinetic energy of Au atoms can be well described in the classical limit and is very close to $\frac{3}{2}kT$ (37 meV). Using such a value for the kinetic energy and a recoil energy of 0.4 eV for Au, results using Eq. (2) in an intrinsic width (σ) of 0.14 eV at 40 keV and hence the lower limit of an elastic peak width for Au (with infinite good experimental resolution) is about 0.33 eV FWHM, whereas the observed width is close to 0.5 eV FWHM. Thus for Au the resolution and intrinsic width contribute about equally to the observed width.

The spectrum obtained after Au evaporation is shown in Fig. 3. The spectrum was fitted in terms of the kinetic energy of the atoms, their masses and the energy resolution. The intensity ratio of the Ti and O peak was fixed to the ratio calculated from ELSEPA. The Au intensity was a free fitting parameter. As the intrinsic width of the Au peak was kept fixed to the value corresponding to a kinetic energy of $\frac{3}{2}kT$, the Au peak allows for the determination of the experimental resolution. From fits of the Ti and O peak we can then deduce their mean kinetic energies from their intrinsic widths. The Ti and O peak are considerable broader than the Au peak and the contribution of the experimental resolution to the observed width is small, and easily corrected for. In this way we get an intrinsic width (σ) of 0.33 eV for Ti (corresponding to $\overline{E_{kin}} = 50$ meV) and 0.062 eV for O (corresponding to $\overline{E_{kin}} = 60$ meV). From these estimates the value of σ_{extra} is 0.53 eV, in reasonable agreement to the value of 0.51 eV used in the O subtraction analysis.

For the spectrum after O subtraction, as shown in Fig. 1 the ambiguity in the energy loss of the electronic excitations has been removed, as now all remaining counts are after backscattering from a Ti atom. The Ti elastic peak position is now taken as the zero loss (due to electronic excitations) position and the 40 keV spectrum can be treated as an ordinary REELS spectrum to determine the dielectric function. At these high energies the surface plasmon contribution (proportional to the time of the surface crossing i.e. $1/(\cos\theta\sqrt{E})$ [13]) is minor and, as was demonstrated for HfO_2, different analysis methods result in very similar estimates of the dielectric function [5].

We used here the Tougaard–Yubero method to extract the dielectric function. As a first step the normalised loss distribution is obtained using the Tougaard–Chorkendorff procedure [14],

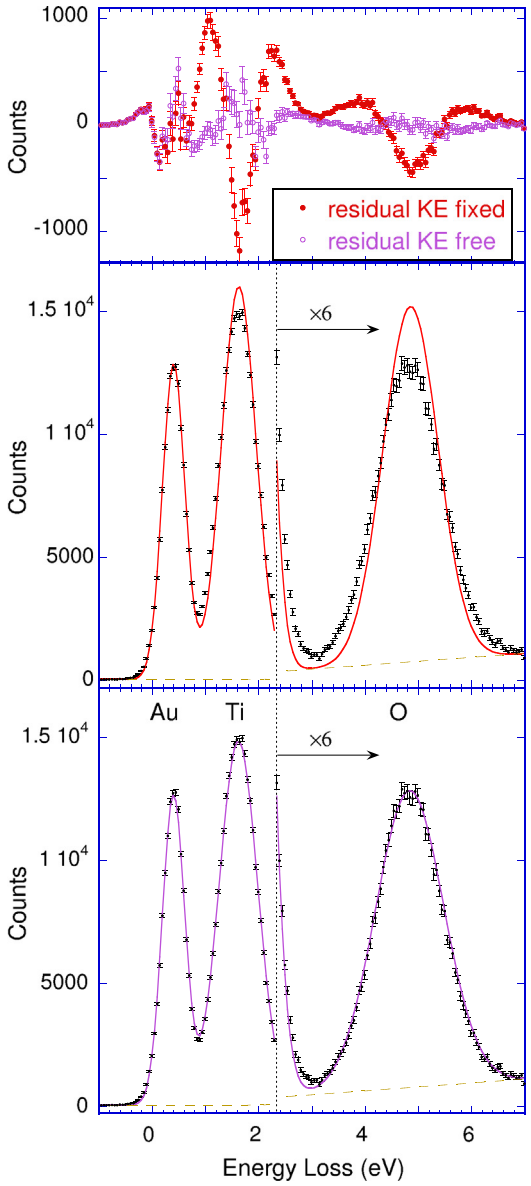

Fig. 3. A spectrum (dots) of a TiO_2 film on which ≈2 Å of Au was deposited. The Au signal is used to determine the resolution of the spectrometer. The larger widths of the Ti and O peak are due to Doppler broadening. In the central panel we calculated a fit based on an intrinsic width corresponding to a mean kinetic energy of $\frac{3}{2}kT$ for the O and Ti atoms. The dashed line is the assumed background. In the lower panel we varied their kinetic energy in order to get the best fit, and values of 50 meV for Ti and 60 meV for O were obtained. The top panel shows the residuals of both fits.

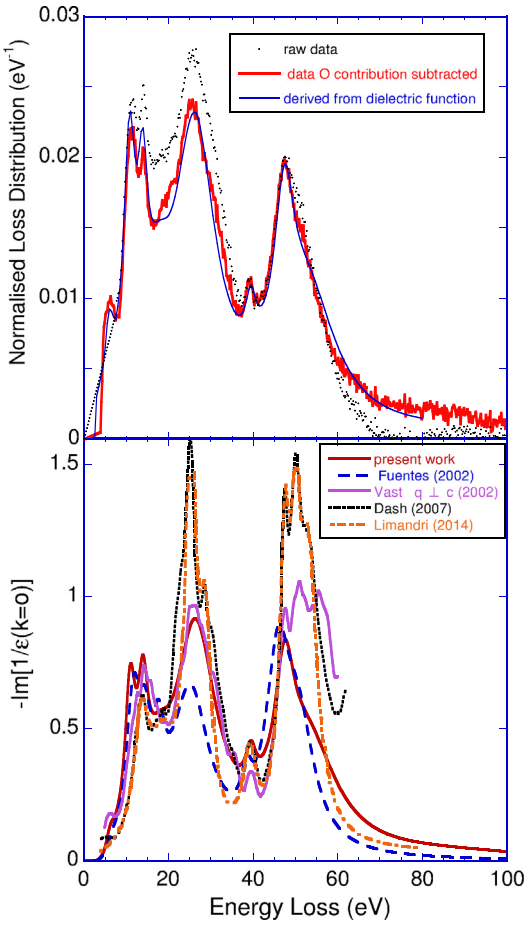

Fig. 4. The top panel shows the normalised loss function as obtained from the experimental data by applying the Tougaard Chorkendorff deconvolution procedure for multiple scattering [14] as applied to the raw data (dots) and after correcting for the shifted contribution of electrons scattered elastically from O. The minor differences visible in the REELS spectra (see Fig. 1) are amplified by this deconvolution procedure. The corrected loss function was fitted with a dielectric function using the QUASES-REELS package. The fit is shown as a solid line. The lower panel shows the present loss function in the optical limit, which is compared with other loss function obtained by Fuentes et al. [16], Vast et al. [17], Dash et al. [18] and Limandri et al. [19].

which corrects for multiple scattering. The result is shown in Fig. 4 using either a raw spectrum as input, or a spectrum after subtraction of the electrons scattered elastically from O. The small differences seen in the input data for this procedure (see Fig. 1) are amplified in the normalised loss distribution. This shows that it is indeed important to correct first for these recoil-induced changes in the spectrum before extracting the loss function. Subsequently the normalised loss function was fitted using the QUEELS program [15], assuming it can be written as a set of n Drude–Lindhard oscillators with energy ω_i, intensity A_i and width γ_i:

$$\mathrm{Im}\left[-\frac{1}{\epsilon(\omega,\mathbf{k})}\right] = \theta(\hbar\omega - E_{\mathrm{gap}})\sum_i^n \frac{A_i\gamma_i\hbar\omega}{\left[(\hbar\omega_i)^2 - \hbar^2\omega^2\right]^2 + (\hbar^2\omega\gamma_i)^2} \quad (4)$$

The obtained fit is shown as well in Fig. 4 and the parameters used are reproduced in Table 2. The lower panel of Fig. 4 shows the loss function in the optical limit ($k = 0$) obtained from the fit and compared to other estimates of this quantity. Note that there is a fair resemblance in the shape of the normalised loss distribution and the loss function of the derived dielectric function in the optical limit. This is not surprising, as the surface loss contribution are relatively minor at the high electron energies used here.

Finally we want to show how the technique described here can be used in a materials science context and we chose for this the topic of preferential sputtering. The TiO_2 layer was sputtered by a 2 keV Ar^+ beam. A 1 μA beam (10 mm Full width half maximum) was applied at normal incidence for 30 min. This results in preferentially removal of oxygen atoms. The surface layer evolves into a non-stoichiometric oxide film. As can be seen in Fig. 5 this results in a reduction of relative strength of the oxygen signal in the elastic peak spectrum taken at 40 keV. For spectra taken at $E_0 = 5$ keV, where the recoil energy is not resolved, there appears to be also a change in shape near the elastic peak. The latter observation has been reported before [20,21]. In sub-stoichiometric TiO_x some Ti 3d levels are occupied, whereas in TiO_2 all Ti 3d levels are empty. The tail observed at the high energy-loss side of the elastic peak of

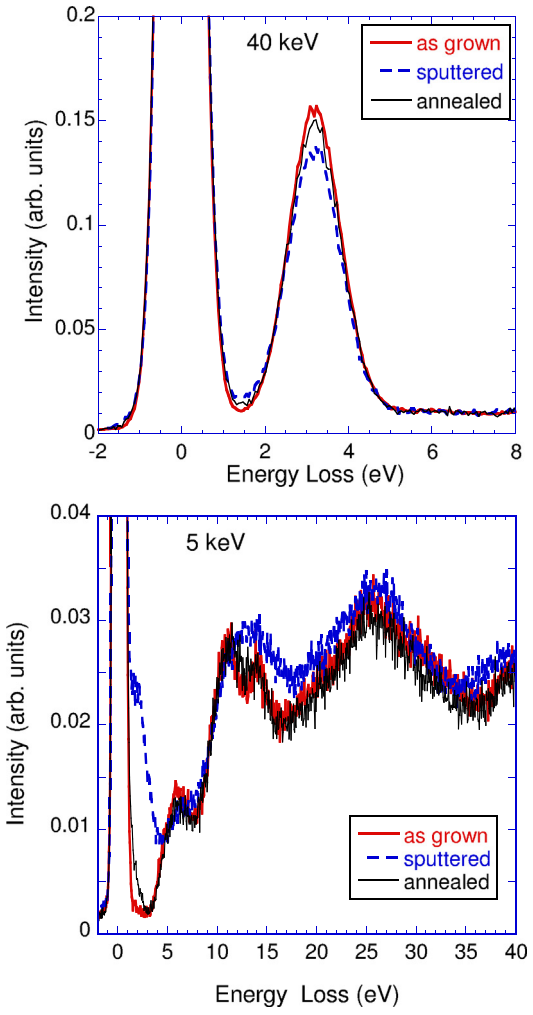

Fig. 5. The top panel shows for a measurement with $E_0 = 40$ keV the elastic peaks of a TiO_2 layer as grown (red, thick line), after sputtering (dashed) and after sputtering plus annealing (black, thin line). The Ti elastic peak (aligned with 0 eV energy loss) was normalised to unit area. Clearly the area of the O elastic peak is decreased after sputtering, but recovers almost completely after annealing. The bottom panel shows a spectrum taken with $E_0 = 5$ keV. Here the elastic peaks are not resolved, but after sputtering extra intensity is seen very close to the elastic peak due to inelastic excitations associated with the Ti^{3+} ions. This intensity decreases after annealing when the film stoichiometry is recovered.

sub-stoichiometric TiO_x is attributed to the excitation of these Ti 3d electrons to higher 3d levels. After annealing near 600 °C the O elastic peak intensity recovers almost completely its original value and at the same time the additional energy loss feature is reduced by an order of magnitude. Correlating electronic structure and elemental composition measurements done in the same spectrometer on a single sample is one of the charming aspects of the experiments described here.

6. Discussion

6.1. Analysis procedure

We have demonstrated here a somewhat different way of analysing spectra of electron scattering experiments where the recoil from different elements is resolved. This procedure subtracts the intensity due to scattering from the light element from the spectrum and can only be applied for *homogeneous* samples. Assuming that the DCS is correctly determined by a program such as ELSEPA, then the analysis procedure has only two unknowns (the relative concentration and the extra width). In contrast to a more traditional fitting procedure (such as described e.g. in Ref. [22]), where a background is affecting the fitting procedure in a less controlled way, the validity of the subtraction procedure can be judged by comparing the spectrum after subtraction with an energy loss spectrum taken at much lower incoming energy. The additional advantage, important when measuring samples for which more than one elastic peak contribute significantly to the spectrum, is that the energy loss spectrum is also corrected for contributions with different recoils. Although this appears at first sight to be only a minor correction, these small differences are amplified when one converts the REELS spectrum to a normalised scattering distribution. This correction is thus required if one wants to extract the dielectric function in these cases.

6.2. Elastic scattering cross sections

For the HfO_2 case we have shown before that for E_0 values as used here the cross section of high-Z elements (such as Hf) is enhanced relative to the Rutherford cross section [4]. It was discussed that this enhancement is intimately related to the difference in stopping of a particle and its antiparticle, a phenomenon that is referred to as the Barkas effect [23,24]. For lighter atoms, such as Ti, the effect is considerable smaller (10% for Ti, compared to 100% for Hf). However, the signal strength of the electrons scattered from O is only about a factor of 4 smaller that the signal strength from Ti, whereas for HfO_2 this difference is close to a factor of 100. It is much more difficult to measure a small O peak adjacent to a huge Hf peak, than to measure an O peak next to a more modest Ti peak. Thus, although the deviation from Rutherford cross section for Ti in TiO_2 is much smaller than that for Hf in HfO_2, this deviation is still well resolved as the Ti:O intensity ratio can be measured with greater precision.

6.3. Elastic peak width and kinetic energy of Ti and O

The phonon structure of TiO_2 is well studied, see e.g. [25,26]. The lower frequency (acoustic) branches are mainly due to motion of Ti atoms whereas the higher frequency optical branches involve mainly the motion of O atoms. Based on this, it is to be expected that the O atoms have more kinetic energy in TiO_2 compared to the Ti atoms. The average atomic kinetic energy, as we claim to measure here, is generally not calculated as part of a phonon calculation. The GULP program has an option to do this [27]. The validity of the output produced by such a program will depend firstly on the appropriateness of the inter-atomic potential used. We run the program using a series of standard potentials for oxides available in the literature [28–31]. Significant differences in the calculated kinetic energies were obtained as can be seen in Table 3. The phonon density of states can be calculated as well using this program. For those potentials where the phonon density of states

Table 2
Drude–Lindhard parameters used in Eq. (4) for the fit in Fig. 4.

ω_i (eV)	A_i (eV^2)	γ_i (eV)
6.2	1.65	2.4
11	16.8	3
14	17.9	3
18	25.5	7
27	266.9	12
39.5	16.6	3
47.5	124	5.5
53.5	366	17
90	102	50

Table 3
The experimental lattice parameters (a and c: unit cell dimensions, x refers to the position of O as a fraction of a, the bulk modules (taken from Ref. [33]) and the kinetic energies of Ti and O as determined in this paper). The same values were calculated using the GULP program for 4 different versions of the Ti^{4+}–O^{2-} potential. Note that these inter-atomic potentials where not designed for the current problem of the determination of the mean kinetic energies of atoms.

	a (Å)	c Å	x fract.	blk md (GPa)	E_{kin} Ti (meV)	E_{kin} O (meV)
exp.	4.59	2.96	0.306	210	50	60
[28]	4.45	3.08	0.312	374	58	69
[29]	4.57	3.16	0.314	160	47	52
[30]	4.57	3.27	0.310	233	50	50
[31]	4.42	3.06	0.305	453	52	54

extended to higher energies larger values of the kinetic energy of the atoms was found. The potentials of [28] gave a phonon density of states that resembles in shape the experimental one [25] most (although it extended to slightly larger energies) and this potential gave a kinetic energy of 60 meV for Ti and 70 meV for O, compared to the experimental values of 50 meV and 60 meV respectively. As the phonon density of states calculated with this potential extends to too high an energy these values should be seen as an upper limit. Comparing high-quality calculations of the mean kinetic energy, based on a fit of experimental phonon dispersion data of constituent atoms in materials such as TiO_2 and SiO_2, would be of great use to test our understanding of both electron scattering and lattice vibrations. Surprisingly, very few theoretical estimates of the mean kinetic energy of atoms exist.

The only previous experimental determination of the mean kinetic energy of atoms in TiO_2 was only for the Ti atoms and based on nuclear resonant photon scattering by Jacob et al. [32]. It assumes the Ti vibrational properties can be described by a Debye model for the phonon density of states (and the oxygen atoms contribute exclusively to the optical branch of the phonon spectrum). In this way a mean kinetic energy at room temperature of 44 meV is obtained. The more recent work of Ref. [26] indicates that for a large part of the phonon spectrum both Ti and O atoms contribute, in contrast to the assumption made by Jacob et al.

6.4. Dielectric function

After correcting for the double elastic peak we determined the dielectric function using the method of Yubero–Tougaard. The resulting normalised loss distribution revealed a wealth of structure. The dielectric function required to fit this loss distribution shows both significant differences and similarities with previous determinations. The agreement with other measurements and calculations on the position of the various peaks in $\mathrm{Im}[-1/\epsilon(\omega, k=0)]$ is quite good, but the intensities differ considerably. The cause of these discrepancies is not fully understood.

6.5. Preferential sputtering

Preferential sputtering is a well established phenomenon, but it is more difficult to determine over which depth range the change in stoichiometry occurs. Is it restricted to the outermost layer, or extends all the way over the penetration depth of the sputtering ion? More elaborate measurements using the technique described here could shed light on this question. Especially for smooth TiO_2 films, it should be possible to measure the O concentration versus depth by changing the geometry (increasing the depth sensitivity by making either the incoming or outgoing trajectory glancing) or by reducing the incoming energy E_0. Such investigations are now under way. The inelastic mean free path of 40 keV electrons is ≈450 Å [34] and hence the mean depth probed in the current geometry (determined by the incoming plus outgoing path length, here the incoming beam was along the surface normal) is of the order of 180 Å. The fact that we observe a sizable depletion of oxygen (≈10%) implies that the O depletion is either very large at the surface, or extends to a significant depth. The present observation of sizeable O deficiencies in measurements that probe rather deep in the material seems to indicate that the O depletion extends past the region probed by XPS, Auger and lower-energy EELS measurements [35–37].

7. Conclusion

We used TiO_2 films as an example to demonstrate that electron scattering at multiple keV energies can be used to study a range of phenomena. The main drawcard of this approach is that the elastic peak provides information about the sample composition and the spectrum at larger energy losses provide information about the electronic structure. In practise we find this method very useful for characterising films of transition metal oxides whose properties are currently being explored extensively for the fabrication of new electronic devices.

Acknowledgements

This work was made possible by a grant of the Australian Research Council. P.L.G. acknowledges the Brazilian agency CAPES (proc. 102209/12-3) for the financial support. The authors want to thank Dr. D. Venkatachalam for performing the thermal oxidation of the Ti foil end Prof. E. Weigold for critically reading the manuscript.

References

[1] M. Vos, Observing atom motion by electron-atom Compton scattering, Phys. Rev. A 65 (2001) 12703.
[2] M. Went, M. Vos, Rutherford backscattering using electrons as projectiles: underlying principles and possible applications, Nucl. Instr. Meth. Phys. Res. Sect. B 266 (2008) 998–1011.
[3] P.L. Grande, M. Vos, D.K. Venkatachalam, S.K. Nandi, R.G. Elliman, Determination of thickness and composition of high-k dielectrics using high-energy electrons, Appl. Phys. Lett. 103 (2013) 071911.
[4] P.L. Grande, M. Vos, Exploring the Barkas effect with keV-electron scattering, Phys. Rev. A 88 (2013) 052901.
[5] M. Vos, P. Grande, The relation between the electron energy loss spectra of hafnia and its dielectric function, Surf. Sci. 630 (2014) 1–8.
[6] M. Vos, R. Moreh, K. Tőkési, The use of electron scattering for studying atomic momentum distributions: the case of graphite and diamond, J. Chem. Phys. 135 (2011) 024504.
[7] V.F. Sears, Scaling and final state interaction in deep inelastic neutron scattering, Phys. Rev. B 30 (1) (1984) 44.
[8] G.I. Watson, Neutron Compton scattering, J. Phys. Condens. Matter 8 (1996) 5955.
[9] F. Salvat, A. Jablonski, C.J. Powell, ELSEPA—Dirac partial-wave calculation of elastic scattering of electrons and positrons by atoms, positive ions and molecules, Comput. Phys. Commun. 165 (2005) 157–190.
[10] M. Vos, M.R. Went, Effects of bonding on the energy distribution of electrons scattered elastically at high momentum transfer, Phys. Rev. B 74 (2006) 205407.
[11] M. Vos, Electron scattering at high momentum transfer from methane: analysis of line shapes, J. Chem. Phys. 132 (2010) 074306.
[12] M. Vos, E. Weigold, R. Moreh, Elastic electron scattering from water vapor and ice at high momentum transfer, J. Chem. Phys. 138 (2013) 044307.
[13] R.F. Egerton, Electron Energy-loss Spectroscopy in the Electron Microscope, Plenum Press, New York, 1996.
[14] S. Tougaard, I. Chorkendorff, Differential inelastic electron scattering cross sections from experimental reflection electron-energy-loss spectra: application to background removal in electron spectroscopy, Phys. Rev. B 35 (1987) 6570–6577.
[15] F. Yubero, S. Tougaard, Quantitative analysis of reflection electron energy-loss spectra, Surf. Interface Anal. 19 (1992) 269–273.
[16] G.G. Fuentes, E. Elizalde, F. Yubero, J.M. Sanz, Electron inelastic mean free path for Ti, TiC, TiN and TiO_2 as determined by quantitative reflection electron energy-loss spectroscopy, Surf. Interface Anal. 33 (2002) 230.
[17] N. Vast, L. Reining, V. Olevano, P. Schattschneider, B. Jouffrey, Local field effects in the electron energy loss spectra of rutile TiO2, Phys. Rev. Lett. 88 (2002) 037601.

[18] L. Dash, F. Bruneval, V. Trinit, N. Vast, Reining, Electronic excitations: ab initio calculations of electronic spectra and application to zirconia ZrO_2, titania TiO_2 and cuprous oxide Cu_2O, Comput. Mater. Sci. 38 (2007) 482.
[19] S. Limandri, R. Fadanelli, M. Behar, L. Nagamine, Fernandez-Varea, I. Abril, R. Garcia-Molina, C. Montanari, D.M.J. Aguiar, J.E. Miraglia, N. Arista, Stopping cross sections of TiO_2 for H and He ions, Eur. Phys. J. D 68 (2014) 194.
[20] Y. Chung, W. Lo, G. Somorjai, Low energy electron diffraction and electron spectroscopy studies of the clean (110) and (100) titanium dioxide (rutile) crystal surfaces, Surf. Sci. 64 (1977) 588.
[21] G. Rocker, J. Schaefer, W. Göpel, Localized and delocalized vibrations on TiO_2(110) studied by high-resolution electron-energy-loss spectroscopy, Phys. Rev. B 30 (1984) 3704.
[22] M. Vos, K. Tokesi, I. Benko, The potential of materials analysis by electron Rutherford backscattering as illustrated by a case study of mouse bones and related compounds, Microsc. Microanal. 19 (2013) 576.
[23] W.H. Barkas, W. Birnbaum, F.M. Smith, Mass-ratio method applied to the measurement of l-meson masses and the energy balance in pion decay, Phys. Rev. 101 (1956) 778–795.
[24] L.H. Andersen, P. Hvelplund, H. Knudsen, S.P. Möller, J.O.P. Pedersen, E. Uggerhöj, K. Elsener, E. Morenzoni, Measurement of the Z_1^3 contribution to the stopping power using mev protons and antiprotons: the Barkas effect, Phys. Rev. Lett. 62 (1989) 1731–1734.
[25] J. Traylor, H. Smith, R. Nicklow, M. Wilkinson, Lattice dynamics of rutile, Phys. Rev. B 3 (1971) 3457.
[26] I. Lukačević, S.K. Gupta, P.K. Jha, D. Kirin, Lattice dynamics and Raman spectrum of rutile TiO_2: the role of soft phonon modes in pressure induced phase transition, Mater. Chem. Phys. 137 (1) (2012) 282.
[27] J. Gale, Gulp: capabilities and prospects, Z. Kristallogr. 220 (5/6/2005) (2005) 552.
[28] S.M. Woodley, P.D. Battle, J.D. Gale, C. Richard, A. Catlow, The prediction of inorganic crystal structures using a genetic algorithm and energy minimisation, Phys. Chem. Chem. Phys. 1 (1999) 2535.
[29] A. Jentys, C. Catlow, Structural properties of titanium sites in Ti-ZSM5, Catal. Lett. 22 (1993) 251–257.
[30] G.C. Mather, M.S. Islam, F.M. Figueiredo, Atomistic study of a catio3-based mixed conductor: defects, nanoscale clusters, and oxide-ion migration, Adv. Funct. Mater. 17 (2007) 905.
[31] C.L. Olson, J. Nelson, M.S. Islam, Defect chemistry, surface structures, and lithium insertion in anatase tio 2, J. Phys. Chem. B 110 (2006) 9995.
[32] I. Jacob, R. Moreh, O. Shahal, A. Wolf, Effective and Debye temperatures of Ti in TiC, TiO_2, and TiH_2, Phys. Rev. B 35 (1987) 8.
[33] J. Muscat, V. Swamy, N. Harrison, First-principles calculations of the phase stability of TiO_2, Phys. Rev. B 65 (2002) 224112.
[34] S. Tanuma, C.J. Powel, D.R. Penn, Calculation of electron inelastic mean free paths, Surf. Interface Anal. 20 (1993) 77–89.
[35] H.J. Mathieu, Beam effects in auger electron spectroscopy analysis of titanium oxide films, J. Vacuum Sci. Technol. 14 (1977) 1023.
[36] W. Göpel, J. Anderson, D. Frankel, M. Jaehnig, K. Phillips, J. Schfer, G. Rocker, Surface defects of TiO_2(110): a combined XPS, XAES and ELS study, Surf. Sci. 139 (1984) 333–346.
[37] J. Malherbe, S. Hofmann, J. Sanz, Preferential sputtering of oxides: a comparison of model predictions with experimental data, Appl. Surf. Sci. 27 (1986) 355.